Table 1

Diffraction data statistics for crystal of rTbgGK

Values in parentheses are for the highest resolution shell.

Space group	$P2_12_12_1$
Unit-cell parameters (Å)	$a = 63.84$, $b = 121.50$, $c = 154.59$
V_M* (Å^3 Da^{-1})	2.5
Solvent content* (%)	50
X-ray source	BL41XU (SPring8)
Wavelength (Å)	1.000
Temperature (K)	100
Resolution (Å)	50 – 2.75 (2.85 – 2.75)
Total reflections	135,987
Unique reflections	31,848
Completeness (%)	97.1 (95.7)
R_{merge} I (%)**	5.5 (46.1)
I/σ	18.4 (3.0)

*Assuming two molecules in the asymmetric unit.

**R_{merge} $(I) = \Sigma_{hkl} \Sigma_i |I_i(hkl) - \langle I(hkl) \rangle| / \Sigma_{hkl} \Sigma_i I_i(hkl)$, where $I_i(hkl)$ is the intensity of the ith observation of reflection hkl and $\langle I(hkl) \rangle$ is their average.

Figure captions

Figure 1

12.5% SDS-PAGE gel stained with Coomassie Brilliant Blue R-250 showing the apparent homogeneity of the purified rTbgGK. Lane 1, molecular weight marker (kDa); lane 2, rTbgGK purified by affinity chromatography on Ni-NTA and gel filtration on Superdex 200

Figure 2

Crystals of rTbgGK obtained by the sitting-drop vapour-diffusion method using PEG 400 as a precipitant.

Figure 3

A typical X-ray diffraction pattern of rTbgCK crystals. The detector edge corresponds to 2.4 Å resolution and an enlarged image of the indicated area around 2.75 Å resolution is shown. The exposure time was 1 s with the oscillation angle of 1.0°.

Figure 1, Balogun *et al.*

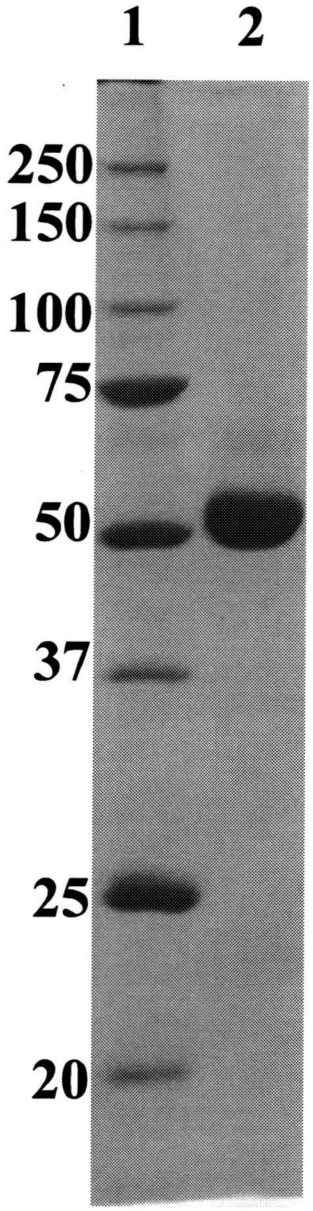

Figure 2, Balogun *et al.*

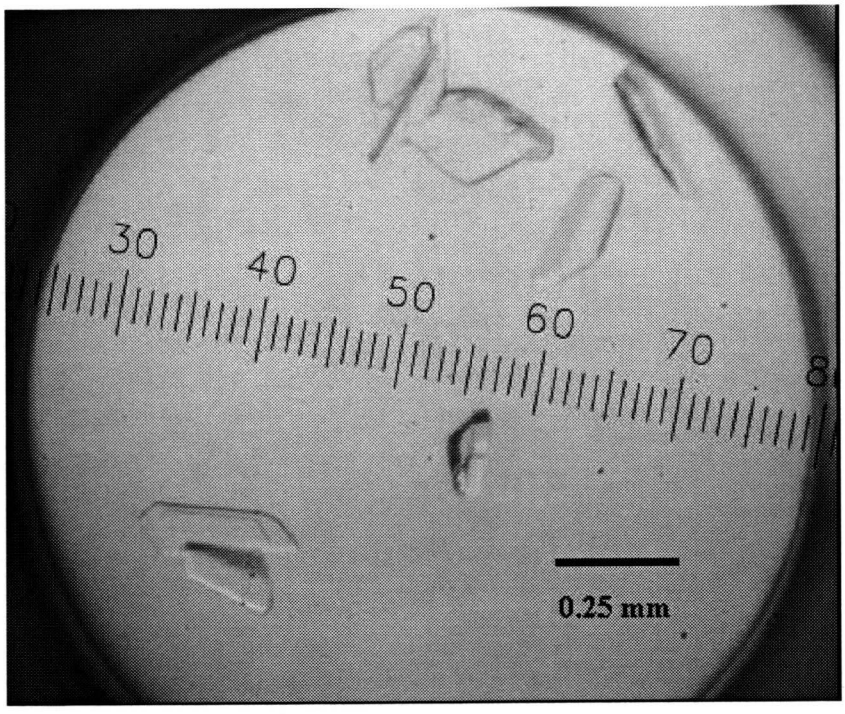

Figure 3, Balogun *et al.*

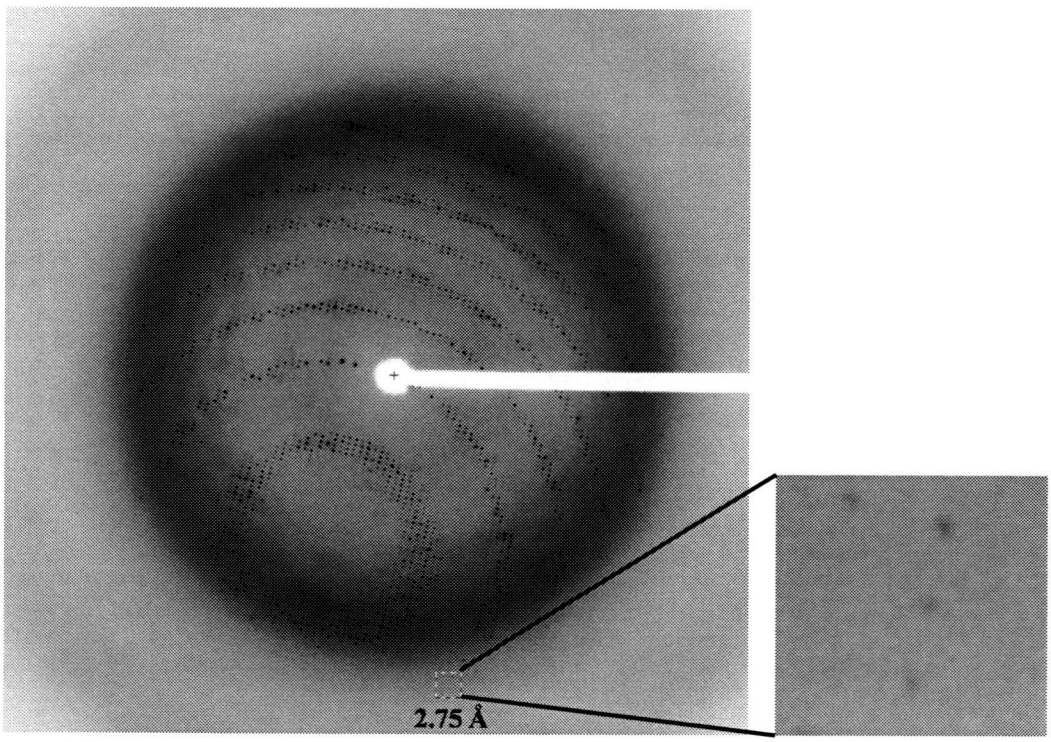

Biochimica et Biophysica Acta 1797 (2010) 443–450

Contents lists available at ScienceDirect

Biochimica et Biophysica Acta

journal homepage: www.elsevier.com/locate/bbabio

Purification and kinetic characterization of recombinant alternative oxidase from *Trypanosoma brucei brucei*

Yasutoshi Kido [a], Kimitoshi Sakamoto [a], Kosuke Nakamura [a], Michiyo Harada [a], Takashi Suzuki [b], Yoshisada Yabu [b], Hiroyuki Saimoto [c], Fumiyuki Yamakura [d], Daijiro Ohmori [d], Anthony Moore [e], Shigeharu Harada [f], Kiyoshi Kita [a,*]

[a] *Department of Biomedical Chemistry, Graduate School of Medicine, The University of Tokyo, Tokyo 113-0033, Japan*
[b] *Department of Molecular Parasitology, Graduate School of Medical Sciences, Nagoya City University, Nagoya 467-8601, Japan*
[c] *Department of Materials Science, Faculty of Engineering, Tottori University, Tottori, Japan*
[d] *Department of Chemistry, School of Medicine, Juntendo University, Tokyo, Japan*
[e] *Biochemistry and Biomedical Sciences, School of Life Sciences, University of Sussex, Falmer, Brighton, UK*
[f] *Department of Applied Biology, Graduate School of Science and Technology, Kyoto Institute of Technology, Kyoto 606-8585, Japan*

ARTICLE INFO

Article history:
Received 24 September 2009
Received in revised form 23 December 2009
Accepted 25 December 2009
Available online 4 January 2010

Keywords:
Alternative oxidase
Membrane-bound diiron protein
Trypanosoma brucei
Ascofuranone
Chemotherapy

ABSTRACT

The trypanosome alternative oxidase (TAO) functions in the African trypanosomes as a cytochrome-independent terminal oxidase, which is essential for their survival in the mammalian host and as it does not exist in the mammalian host is considered to be a promising drug target for the treatment of trypanosomiasis. In the present study, recombinant TAO (rTAO) overexpressed in a haem-deficient *Escherichia coli* strain has been solubilized from *E. coli* membranes and purified to homogeneity in a stable and highly active form. Analysis of bound iron detected by inductively coupled plasma-mass spectrometer (ICP-MS) reveals a stoichiometry of two bound iron atoms per monomer of rTAO. Confirmation that the rTAO was indeed a diiron protein was obtained by EPR analysis which revealed a signal, in the reduced forms of rTAO, with a g-value of 15. The kinetics of ubiquiol-1 oxidation by purified rTAO showed typical Michaelis–Menten kinetics (K_m of 338 μM and V_{max} of 601 μmol/min/mg), whereas ubiquinol-2 oxidation showed unusual substrate inhibition. The specific inhibitor, ascofuranone, inhibited the enzyme in a mixed-type inhibition manner with respect to ubiquinol-1.

© 2009 Elsevier B.V. All rights reserved.

1. Introduction

Trypanosoma brucei is a parasite that causes African sleeping sickness in humans and Nagana in livestock and is transmitted by the tsetse fly. There is an urgent need for further development of chemotherapy against African trypanosomiasis since current chemotherapeutic drugs are not entirely satisfactory [1].

Trypanosomal parasites are equipped with a unique energy metabolism, they live as the bloodstream form in the mammalian host and as the procyclic form in the vector. The procyclic form of *T. brucei* fulfills its ATP requirement from a cyanide-sensitive and cytochrome-dependent respiratory chain comparable to that observed in the host mitochondria, whereas in the bloodstream form, trypanosomes use the glycolytic pathway, which is localized in a unique organelle the glycosome, as their major source of ATP [2–5]. Once the parasites invade the mammalian host in the bloodstream form, both its cytochrome-dependent respiratory chain and ATP synthesis by oxidative phosphorylation disappear [2,5]. Instead a cyanide-resistant and cytochrome-independent trypanosomal alternative oxidase (TAO) functions as the sole terminal oxidase to re-oxidize NADH accumulated during glycolysis [5].

TAO is generally considered to be a good target for the anti-trypanosomal drugs because this oxidase is essential for their survival, since it reoxidises cytosolic NADH, and mammalian hosts do not possess this protein [5,6]. Indeed, we found that ascofuranone, isolated from the pathogenic fungus *Ascochyta visiae*, specifically inhibits the quinol oxidase activity of TAO and rapidly kills the parasites [7]. In addition, we have confirmed the chemotherapeutic efficacy of ascofuranone *in vivo* [8,9].

The alternative oxidase (AOX) is a non-protonmotive ubiquinol oxido-reductase catalyzing the 4-electron reduction of dioxygen to water [5,10–12]. Genes encoding AOX have been found in higher

Abbreviations: AOX, alternative oxidase; DM, *n*-dodecyl-β-D-maltopyranoside; EPR, electron paramagnetic resonance; ICP-MS, inductively coupled plasma-mass spectrometer; IPTG, isopropyl, β-D-1-thiogalactoside; k_{cat}, molecular activity; C10E8, octaethylene glycol-monododecylether; OG, *n*-octyl-β-D-glucopyranoside; rTAO, recombinant trypanosome alternative oxidase; SHAM, salycylhydroxamic acid; TAO, trypanosome alternative oxidase; Ubiquinol, reduced form ubiquinone

* Corresponding author. Department of Biomedical Chemistry, Graduate School of Medicine, The University of Tokyo, Hongo, Bunkyo-ku, Tokyo 113-0033, Japan. Tel.: +81 3 5841 3526; fax: +81 3 5841 3444.
E-mail address: kitak@m.u-tokyo.ac.jp (K. Kita).

0005-2728/$ - see front matter © 2009 Elsevier B.V. All rights reserved.
doi:10.1016/j.bbabio.2009.12.021

plants, algae, yeast, slime molds, free-living amoebae, eubacteria and nematodes [13–16]. Moreover, recent bioinformatic searches have broadened the taxonomic distribution of AOX to some members of the animal kingdom [17]. The primary role of AOX in non-thermogenic plants is to regulate cellular redox balance and to protect against reactive oxygen species particularly when the cytochrome pathway is inhibited [18–20]. In addition to this role, many other physiological roles have been described for AOXs in other organisms and these have been discussed in detail elsewhere [13,21]. The ubiquitous occurrence of AOX may suggest that the metabolic flexibility that the alternative pathway confers upon an organism allows it to respond to a wide range of developmental and environmental conditions [22].

Despite universal conservation of the gene and diversified physiology, the molecular features of AOX have not yet been well characterized. Although no high-resolution AOX structure has been determined to date, current structural models predict that it is an integral interfacial membrane protein that interacts with a single leaflet of the lipid bilayer, and contains a non-haem diiron carboxylate active site [23,24]. This model is supported by extensive site-directed mutagenesis studies [18,25–29] and furthermore both EPR and FTIR spectroscopies have confirmed the presence of a binuclear iron center in both the plant and trypanosomal enzymes [30–32].

Further detailed structural and biochemical analyses of AOXs, however, requires further development of purification protocols to produce sufficiently purified and highly active protein to enable crystallization trials and kinetic analyses to proceed. In this paper, we report on the further refinement of our previous protocol through over-expressing rTAO in an *E. coli ΔhemA* mutant (FN102) strain, which lacks quinol oxidase activity of cytochrome *bo* and *bd* complexes [33–35]. Purified rTAO protein is highly active and exhibits an exceptional stability upon storage. The analysis of the prosthetic groups by inductively coupled plasma-mass spectrometer (ICP-MS) and electron paramagnetic resonance (EPR) reveals the presence of two ferric ions stoichiometrically bound per rTAO monomer. To our knowledge this is the first direct confirmation of two ferric irons per AOX. Furthermore we show that purified rTAO is potently inhibited by ascofuranone with mixed function kinetics.

2. Materials and methods

2.1. Preparation of membrane sample

The strain FN102/pTbAO carrying cDNA for *T. b. brucei* TAO [36] was pre-cultured at 37 °C in 100 ml of LB medium containing 10 mg ampicillin, 5 mg kanamycin, and 5 mg 5-aminolevulinic acid for 4–6 h. The pre-cultured cells were aerobically grown at 30 °C in 10 l of S-medium containing 100 g tryptone peptone, 50 g yeast extract, 50 g casamino acid, 104 g K_2HPO_4, 30 g KH_2PO_4, 7.5 g trisodium-citrate·$2H_2O$, 25 g $(NH_4)_2SO_4$, 0.5 g $MgSO_4 \cdot 7H_2O$, 0.25 g $FeSO_4 \cdot 7H_2O$, 0.25 g $FeCl_3$, 0.2%(w/v) glucose, and 1 g carbenicillin. The culture was initiated at O.$D_{600} = 0.01$ and expression of rTAO was induced by the addition of isopropyl β-D-1-thiogalactoside (IPTG) (25 μM) at O.$D_{600} = 0.1$. Cells were harvested 8–10 h following induction and were resuspended in 50 mM Tris–HCl (pH 7.5) containing 20%(w/w) sucrose, 0.1 mM phenylmethane sulfonyl fluoride (PMSF) and protease inhibitor cocktail (Sigma) and broken by a French Pressure Cell (Ohtake, Tokyo). Unbroken cells were removed by centrifugation at 8000 *g* for 10 min (Hitachi 21G). Inner membranes of FN102/pTbAO were fractionated in high density sucrose after ultracentrifugation at 200,000 *g* for 1 h at 4 °C (Hitachi 85H) (35 ml of supernatant was overlaid over 35 ml of 50 mM Tris–HCl pH 7.5 containing 40%(w/w) sucrose per ultracentrifuge tube). Buoyant inner rich membranes upon 40%(w/w) sucrose layer were fractionated and the inner membrane pellet was separated by further ultracentrifugation at 200,000 *g* for 1 h (HITACHI 85H). The membrane pellet was resuspended in 50 mM Tris–HCl (pH 7.5) containing 20%(w/w) sucrose.

2.2. Solubilization

Membranes were treated with solubilization buffer (6 mg/ml protein in 50 mM Tris–HCl, 1.4%(w/v) *n*-octyl-β-D-glucopyranoside (OG), 200 mM $MgSO_4$, 20%(v/v) glycerol, pH 7.3) at 4 °C and immediately ultracentrifuged at 200,000 *g* for 1 h at 4 °C. The quinol oxidase activities of the samples before centrifugation, as well as that of supernatant and pellet were determined.

2.3. Purification of rTAO

Hybrid batch/column procedure described in the manufacturer's instruction was used as stated below. Ten milliliter of the resin (BD Bioscience, TALON Metal Affinity Resin) was equilibrated in a batch format by 100 ml of equilibration buffer (20 mM Tris–HCl, 1.4%(w/v) OG, 100 mM $MgSO_4$, 20%(v/v) glycerol, pH 7.3). Twenty milliliter of OG extract was mixed with the resin for 20 min at 4 °C. The resin was washed twice with 100 ml of wash buffer (20 mM Tris–HCl, 20 mM imidazole, 0.042%(w/v) *n*-dodecyl-β-D-maltopyranoside (DM), 50 mM $MgSO_4$, 20%(v/v) glycerol pH 7.3) and the resin bound rTAO was transferred to a column for additional washing with 20 ml of second wash buffer (20 mM Tris–HCl, 165 mM imidazole, 0.042%(w/v) DM, 50 mM $MgSO_4$, 20%(v/v) glycerol pH 7.3; flow rate 1 ml/min) and protein elution. Finally, rTAO was eluted with elution buffer (20 mM Tris–HCl, 200 mM imidazole, 0.042%(w/v) DM, 50 mM $MgSO_4$, 60 mM NaCl, 20%(v/v) glycerol pH 7.3; flow rate 1 ml/min). Fractions (4 ml each) were collected.

2.4. Quantitative analysis of metals and EPR spectroscopy

Three independent preparations of rTAO were analyzed (details in Section 3). Each sample solution containing 0.1 g of rTAO was added to 1 ml of nitric acid and 7 ml of water. Organic compounds were hydrolyzed by microwave-assisted protein digestion system (Ethos Pro, Milestone General). Fe, Mn, Cu, Zn and Co in each sample were quantified by inductively coupled plasma-mass spectrometer (ICP-MS, ELAN DRC PerkinElmer Japan). Analysis was performed by the Sumika Chemical Analysis Center (Osaka, Japan). Protein concentration was determined by the Lowry method.

EPR spectra were recorded on a JEOL X-band JES-FA300 spectrometer equipped with an ES-CT470 Heli-Tran cryostat system and a Scientific Instruments digital temperature indicator/controller model 9700a. For EPR analysis of rTAO, 13 mg/ml purified rTAO was frozen in EPR tubes in liquid nitrogen. The purified rTAO was reduced by 2 mM dithionite and 1 mM phenazine methosulfate prior to freezing.

2.5. Ubiquinol oxidase assay

Ubiquinol oxidase activity was measured by recording the absorbance change of ubiquinol-1 at 278 nm (Shimadzu spectrophotometer UV-3000). Reactions were started by the addition of ubiquinol-1 (final concentration 150 μM, $\varepsilon_{278} = 15{,}000\ M^{-1}\ cm^{-1}$) after 2 min preincubation at 25 °C in the presence of rTAO and 50 mM Tris–HCl (pH 7.4). For the enzyme kinetics of purified rTAO, the reaction was initiated by the addition of ubiquinol-1 after 2 min preincubation at 25 °C in the presence of rTAO and 50 mM Tris–HCl (pH 7.4) containing 0.05%(w/v) octaethylene glycol-monododecylether detergent (C10E8).

2.6. Chemicals

All chemicals were biochemistry grade. Ubiquinone-1 and protease inhibitor cocktail were purchased from Sigma-Aldrich. The other detergents were purchased from Dojin Chemicals (Tokyo, Japan).

3. Results

3.1. Purification of fully active TAO

Although we previously established a protocol for the overproduction of rTAO in *E. coli* FN102 (*ΔhemA*) lacking cytochrome *bo* and *bd* complexes of the bacteria, the yield of the active enzyme was too low to analyze its prosthetic group [36]. Such a preparation also hampered the determination of kinetic parameters of rTAO such as its molecular activity. Therefore, conditions for the expression of rTAO and purification protocols were optimized to obtain large quantities of active and stable rTAO to enable such determinations. Three factors were critical to obtain large amounts of active rTAO, namely, growth time of the culture prior to addition of IPTG, absolute concentration of IPTG, and the use of purified inner membranes as the starting material.

After extensive screening of detergents and additives to establish the procedure for efficient extraction of active rTAO from the inner membranes, we found that *n*-octyl-β-D-glucopyranoside (OG) specifically solubilized rTAO as shown in Table 1 (specific activity increased from 23.3 to 63.2 μmol/min/mg after solubilization). Approximately 60% of the membrane quinol oxidase activity was recovered with 1.4%(w/v) OG in the extract (Sup. Fig. 1). Thus, recovery of the activity was significantly higher than that of previously reported digitonin extraction (17%) [36]. Following solubilization, it was possible to maintain enzymatic activity for at least 1 month at 20 °C.

Since rTAO was fused with N-terminal histidine tag, solubilized rTAO was purified by cobalt affinity chromatography. Although the enzyme solubilized by OG was bound to the cobalt affinity resin in the presence of OG, it was not possible to elute bound rTAO from the resin with buffer containing OG. Interestingly, however, we found that 100% of the rTAO activity could be recovered from the column when OG in the washing and elution buffers was exchanged with *n*-dodecyl-β-D-maltopyranoside (DM). In the final step, purified rTAO was obtained by a two-step elution with 165 mM and 200 mM imidazole, which resulted in a very efficient purification of active rTAO in the presence of DM. A typical elution profile of quinol oxidase activity with increasing imidazole concentration is shown in Sup. Fig. 1B. Purified rTAO, with a molecular mass of 34 kDa, was estimated to be 95% pure by SDS-PAGE (Fig. 1A, lane 5). In addition to the 34 kDa band, it is apparent that other bands are also present including two with a smaller size than rTAO and one band with an approximate molecular mass of 74 kDa. Since all of these bands were recognized in Western blot using a monoclonal antibody against TAO (Fig. 1B), the smaller protein bands possibly represent proteolytic breakdown products whilst the 74 kDa band most likely represents the dimeric form of rTAO. The specific activity of purified rTAO was more than 200 μmol/min/mg protein when 150 μM of ubiquinol-1 was used as a substrate, which had a five-fold higher activity than that of the previously purified rTAO (approximately 40 μmol/min/mg) [36]. Quinol oxidase activity of purified rTAO was insensitive to 5 mM KCN but was completely inhibited by 10 nM ascofuranone. A greater than 35-fold increase in purification was achieved using the techniques described above, and 13.2% of the total activity was recovered from the lysate of FN102/pTAO cells as summarized in Table 1. Such procedures resulted in approximately 10 mg of highly purified rTAO from a 10 l culture.

Table 1
Purification of rTAO.

Fractions	Total activity (μmol/min)	Protein (mg)	Specific activity (μmol/min/mg)	Recovery (%)
E. coli lysate	14100	2410	5.85	100
Inner membrane	3500	150	23.3	24.8
OG extract	2400	37.9	63.2	17.0
Co-column	1860	8.95	207	13.2

The activities listed here were measured using 150 μM of ubiquinol-1. Fractions (eluate numbers 6–13 in Supplemental Fig. 1B) were collected as purified rTAO after co-column.

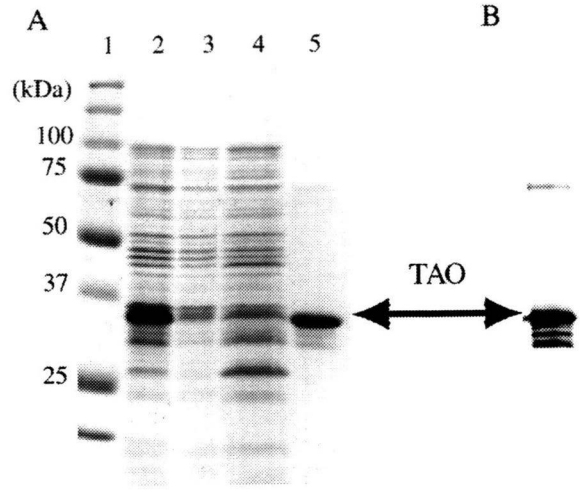

Fig. 1. SDS-PAGE and Western blotting of rTAO in purification steps. A: CBB-staining 12.5% SDS-PAGE of each fraction from the cobalt column chromatography. Lane 1, marker; lanes 2 and 3, each 5 ml of OG extract and flow through fraction; lane 4, 500 ml of wash fraction; and lane 5, 60 ml of eluted fraction collected from fractions 6–12. Loading samples on lanes 2 to 5 were precipitated with acetone. B: Western blot of purified rTAO. The same sample to lane 5 in panel B was electrophoresed on 12.5% polyacrylamide gel. Monoclonal antibodies were used against highly purified rTAO obtained by a nickel column in the presence of guanidine. Epitope recognized by this antibody is the C-terminal domain of the enzyme. The arrow indicates rTAO with an apparent molecular mass of 34 kDa.

3.2. Iron content in purified TAO

Since a highly active and stable purified rTAO could be obtained by the protocol described above, the metal content of purified rTAO was measured by ICP-MS. On the basis that TAO has a diiron center as previously proposed [23,24], then two equivalents of iron should be detected per monomer of rTAO. To this end we analyzed the iron content of purified native rTAO, inactive rTAO, denatured rTAO, and iron within the buffer eluted from the cobalt-column. Purified native rTAOs derived from three independent *E. coli* cultures were precipitated by PEG 3350 and resuspended in the elution buffer at three different concentrations as shown in Sup. Table 1. To prepare inactive rTAO, precipitated rTAO was resuspended in 50 mM Tris–HCl pH 7.4, which resulted in complete loss of enzyme activity. Denatured rTAO was prepared by resuspending the precipitant in elution buffer containing 6 M guanidine–HCl and 0.3 M EDTA. Metal contents in these preparations were 9000 ng/ml, 2900 ng/ml and 1800 ng/ml of Fe respectively for the native rTAO (3.71, 1.19 and 0.80 mg/ml), 230 ng/ml, 100 ng/ml and 28 ng/ml of Fe for inactive rTAO, denatured rTAO and the elution buffer, respectively (Sup. Table 1). From these results, the stoichiometry of bound iron per rTAO monomer can be deduced as indicated below, based on the following parameters namely, a molecular mass of rTAO of 39,391 Da (including the 6× histidine tag), purity of 95% based on SDS-PAGE gels, and the atomic weight of Fe being 55.85. Thus the ratio of iron atoms per rTAO is 1.76 for native rTAO and 0.2 and 0.08 in inactive rTAO and denatured rTAO, respectively (Table 2). This data indicates that one monomer of TAO possesses two atoms of iron which are released during inactivation or denaturation of the enzyme. To our knowledge, this is the first direct measurement of iron in purified AOX and the stoichiometry is consistent with the active site of AOX being a diiron carboxylate-center.

Other metals including Mn, Cu and Zn were also analyzed (Sup. Table 1). In all cases, these metals were below their detection limit (10 ng/ml sample solution) or background level. Although cobalt was

Table 2
Ratio of metals to purified rTAO.

	Fe/rTAO	Zn/rTAO	Mn/rTAO	Cu/rTAO
	Mean ± S.D.			
Native rTAO	1.76 ± 0.077	0.03 ± 0.013	N.D.[a]	N.D.
Inactive rTAO	0.22[b]	N.D.	N.D.	N.D.
Denatured rTAO	0.08[b]	N.D.	N.D.	N.D.

Stoichiometric ratio of metals to one molecular TAO was calculated using data in Supplemental Table 1.
[a] N.D. represents Not Detected (below 0.01).
[b] The value is an average of two independent experiments.

detected in purified rTAO, its concentration was comparable to that of cobalt in the elution buffer derived from the resin (data not shown). Similarly although 130 ng/ml, 66 ng/ml and 61 ng/ml of Zn were detected in native rTAO, these amounts of Zn were not commensurate with that of the enzyme stoichiometry. The detected Zn might be derived from the Zn-substituted form of rTAO, which was suggested to be possible from structural analysis [37]. In addition, at least 90% of the purified rTAO retained its prosthetic group in its active form.

In addition to measuring the stoichiometry of iron in purified rTAO, EPR analysis of purified rTAO was also performed in order to confirm that purified rTAO was indeed a diiron carboxylate protein and whether the detected iron originated from a diiron binding center. As shown in Fig. 2, a low field EPR signal at approximately $g = 15$ in the perpendicular EPR mode was observed with the reduced form of rTAO when the enzyme was reduced by 2 mM of dithionite and 1 mM of phenazine methosulfate (PMS), although the intensity of the signal was low. Importantly the signal disappeared in the oxidized form of rTAO. This low field EPR signal is characteristic for diiron proteins and is ascribed to an exchange-coupled high spin ferrous iron [38]. Although this signal is not normally observed in the perpendicular mode, it can be detected under certain conditions as outlined in this report [39]. The effective g-value of 15 observed in the perpendicular mode is slightly lower than the value of 16 previously observed by us [31] but this is probably due to the fact that parallel-mode EPR spectroscopy is a much more sensitive probe than the perpendicular mode. Nevertheless the finding of a low field signal when the purified enzyme is reduced is further confirmation that the purified rTAO we report here is indeed a diiron carboxylate protein. It should be noted however that we were unable to observe the $g = 15$ signal when the enzyme was reduced by more physiological reductants such as ubiquinol-1 the reasons for which are, at present, unclear.

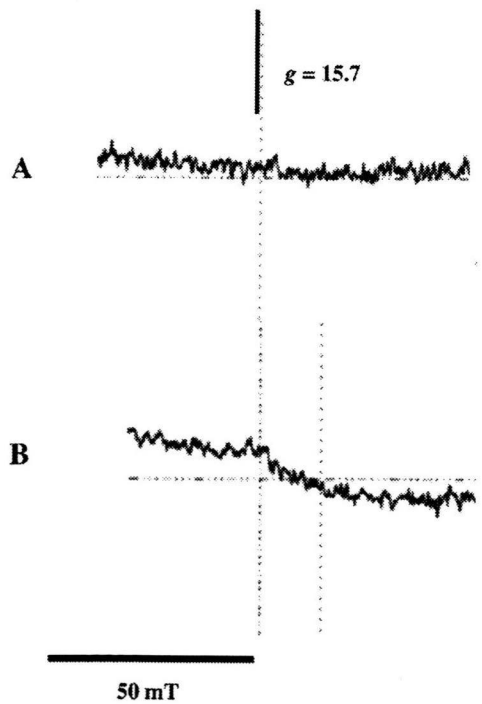

Fig. 2. EPR spectra of rTAO. A: Oxidized form of rTAO (360 μM). B: Reduced form of rTAO (360 μM), which was treated by 2 mM of dithionite and 1 mM phenazine methosulfate for 30 min on ice. Instrument parameters: microwave frequency, 9.02 GHz; microwave power, 1 mW; modulation frequency, 100 kHz; modulation amplitude, 0.6 mT; and temperature of 5 K.

3.3. Kinetic properties of purified TAO

Kinetic analysis of purified rTAO (or AOX) using ubiquinone analogs has previously proved difficult because: 1) the enzyme, following solubilization, was extremely unstable, 2) the natural substrate of trypanosome AOX is ubiquinol-9 [4], which is too hydrophobic to use as the substrate in the assay and 3) the enzymatic activity was not saturated at the maximum concentration of ubiquinol-1 (approximately 300 μM). Since we have purified rTAO in a fully active form and confirmed the stoichiometric presence of the diiron center, the purified rTAO was well-suited to a kinetic analysis.

As noted in our earlier study [36] and in AOXs from other organisms [40] non Michaelis–Menten kinetics is observed when ubiquinol-1 is used as a substrate. Hoefnagel et al. [40], however, observed that the addition of a specific detergent (0.025% EDT-20) during the assay increased the activity by 3- to 4-fold close to saturation. Although the addition of 0.025%(w/v) of EDT-20 equally enhanced the activity of purified rTAO by approximately 2-fold, it did have a deleterious effect upon the long term stability of the enzyme (Sup. Fig. 2).

In an attempt to overcome this problem, various detergents were therefore screened to determine if they could enhance activity without affecting enzyme stability. When the effect of the detergents on enzyme activity was evaluated by monitoring the activity of rTAO in the presence of detergent (Sup. Fig. 3), most activity was retained in the presence of 0.05%(w/v) of C10E8 (Sup. Fig. 4A). Light scattering at 400 nm confirmed that at least 600 μM of ubiquinol-1 was soluble in the assay system (Sup. Fig. 4B). The kinetics of ubiquinol-1 oxidation by purified rTAO in the presence of 0.05%(w/v) of C10E8 showed typical Michaelis–Menten kinetics (Fig. 3, K_m of 338 ± 23.2 μM and V_{max} of 601 ± 27.0 μmol/min/mg). In contrast, activity was linearly dependent upon substrate concentration in the absence of detergent indicating unsaturation in agreement with previous studies [36,40] (Fig. 4). Enzymatic analysis was performed with a wide range of

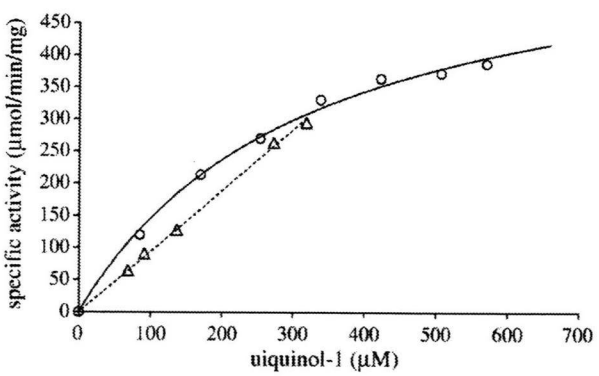

Fig. 3. Kinetics of ubiquinol-1 oxidation by purified rTAO. S–V plot of ubiquinol oxidase activity is shown using 75 ng of purified rTAO in 50 mM Tris-HCl (pH 7.4) and ubiquinol-1 (80–580 μM) with (○) and without (△) 0.05%(w/v) C10E8 at 25 °C. The solid line indicates the fitted Michaelis–Menten kinetics with the detergent (K_m of 338 ± 23.2 μM and V_{max} of 601 ± 27.0 μmol/min/mg), whereas the dashed line indicates the linear relationship between the substrate concentration and the activity without the detergent.

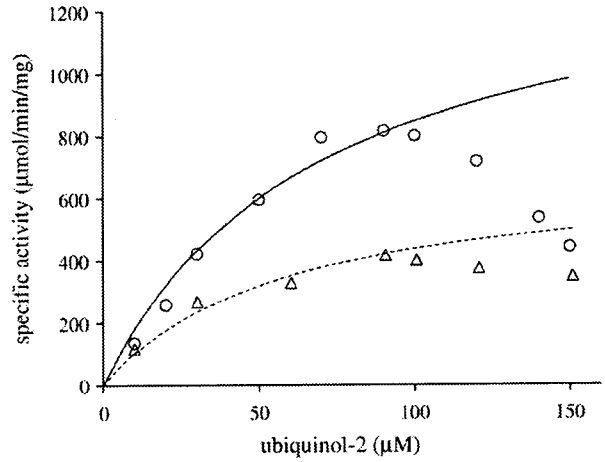

Fig. 4. Kinetics of ubiquinol-2 oxidation by purified rTAO. S–V plot of ubiquinol oxidase activity is shown using 75 ng of purified rTAO in 50 mM Tris–HCl (pH 7.4) and ubiquinol-2 (10–150 μM) with (△) 0.05%(w/v) C10E8 and with (○) 0.025%(w/v) EDT-20 at 25 °C. The solid line indicates the fitted Michaelis–Menten kinetics in the concentration range below 90 μM of ubiquinol-2 with 0.025%(w/v) EDT-20, whereas the dashed line does with 0.05%(w/v) C10E8 (K_m of 71 ± 1.2 μM and V_{max} of 1,460 ± 53.2 μmol/min/mg with 0.025%(w/v) EDT-20, whereas K_m of 57 ± 8.5 μM and V_{max} of 691 ± 28.0 μmol/min/mg with 0.05%(w/v) C10E8).

substrate concentrations (80–570 μM), which corresponded to 0.4 K_m–1.7 K_m.

To investigate whether the length of the side chain of the substrate affected the kinetic properties of rTAO, a kinetic analysis using ubiquinol-2 in the presence of EDT-20 and C10E8 (Fig. 4) was performed. Fig. 4 indicates that during the oxidation of ubiquinol-2, enzyme activity decreased above 100 μM substrate even in buffers containing either detergent. Although kinetic parameters using ubiquinol-2 could not be obtained due to substrate inhibition, S–V plots in the concentration range below 90 μM of ubiquinol-2 could be used to qualitatively analyze the effects of side chain on enzyme activity. Calculated values from such plots revealed that in the presence of 0.025%(w/v) EDT-20 the K_m (ubiquinol-2) was 71 ± 1.2 μM and V_{max} = 1460 ± 53.2 μmol/min/mg whereas with, 0.05%(w/v) C10E8 the K_m was 57 ± 8.5 μM and V_{max} = 691 ± 28.0 μmol/min/mg.

Ascofuranone is a highly specific and potent inhibitor of TAO [7] and it was therefore of importance to determine its inhibitory effect on ubiquinol-1 oxidation by purified rTAO in the presence of 0.05%(w/v) of C10E8 (Sup. Fig. 5A). From the data presented in Sup. Fig. 5A the apparent kinetic parameters of ubiquinol-1 oxidation in the presence of 0.5 nM and 2 nM of ascofuranone were estimated to be respectively $K_m^{0.5\,nM}$ = 368 ± 6.4 μM; $V_{max}^{0.5\,nM}$ = 490 ± 22.4 μmol/min/mg and $K_m^{2\,nM}$ = 492 ± 7.2 μM; and $V_{max}^{2\,nM}$ = 309 ± 60.5 μmol/min/mg. The increased K_m and decreased V_{max} values (Sup. Fig. 5B) indicate that ascofuranone inhibits purified rTAO in a mixed-type non-competitive manner with respect to ubiquinol-1.

4. Discussion

The overall goal of the present study was to obtain a highly pure and stable rTAO protein with maximum specific activity which could be used to investigate the kinetic properties of the enzyme. The quality of the purified rTAO obtained in this study has resulted in three important aspects with respect to the structure of AOX namely, the first direct evidence of stoichiometrically bound iron within the diiron center of rTAO, secondly reliable measurements of kinetic parameters and thirdly that a sample of sufficient purity and yield could be produced that has resulted in the formation of crystals [41].

4.1. Overexpression and purification of rTAO

The difficulties in isolating stable AOXs in an active form have hampered the biochemical and structural analyses of the enzyme including identification of its prosthetic groups, tertiary structural analysis and the definition of enzyme kinetic parameters. The present study reports on the overexpression and purification of active rTAO, which has enabled us to study biochemical and protein chemistry properties of this enzyme. The protocol described in this paper results in the purification of large amounts of stable rTAO with high specific activity. Two factors appeared critical to functionally express highly active rTAO. Firstly, the optimization of culture conditions, including culture duration and IPTG concentration, was crucial for the successful overexpression of rTAO with high specific activity. Secondly, activity was maximized when rTAO was purified from *E. coli* inner membranes—activity decreased substantially when it was isolated from an unpurified membrane fraction. Additionally, changing the detergent from OG to DM following solubilization, also appeared important to maximize yield and activity. Purified rTAO produced in this manner retained complete activity for more than 6 months at 4 °C and for more than 1 month at 20 °C. Furthermore, we have also been able to purify *Sauromattum guttatum* rAOX by this procedure showing the universality of the purification protocol (Elliott, C.E., Kido, Y., Kita, K. and Moore, A.L. unpublished observations).

It is anticipated that highly purified and active AOX will open a new direction with respect to the investigation of the structure and reaction mechanisms of AOXs and contribute to further progress on the study of this novel terminal oxidase. Indeed we recently took advantage of the exceptional stability and purity of the rTAO by performing the first FTIR spectroscopic investigation of any diiron protein [32]. Stepwise reduction of the fully oxidized resting state of rTAO revealed two distinct IR redox difference spectra. The first of these, "signal 1", contained clear features that could be assigned to protonation of at least one carboxylate group, further perturbations of carboxylic and histidine residues, bound ubiquinone and a negative band that might arise from a radical in the fully oxidized protein. A second IR redox difference spectrum, "signal 2", appeared more slowly (within approximately 1 h) once signal 1 had been reduced and is quite distinct from the components which comprise signal 1. The exact identity of the components which result in signal 2 await further investigations. Such a study has not previously been possible with AOX preparations because of protein instability at room temperature.

4.2. Prosthetic group analysis

Prosthetic group analysis summarized in Table 2 revealed that in highly stable and purified rTAO there are two equivalents of iron per rTAO monomer with no other metals, including Cu, Mn and Zn, being detected. EPR spectroscopy confirms that the irons are part of a diiron center since an EPR signal at $g = 15$ could be detected (Fig. 2) when rTAO is reduced by dithionite in the presence of PMS. The fact that this signal can be detected in all AOXs examined to date suggests that the signal is a characteristic signature of AOXs [30,31] and in agreement with mutational analyses [18,25–29] is further confirmation that TAO, similar to AOXs in other organisms, is a diiron carboxylate protein. Furthermore the data summarized in Table 2 revealed that when the protein was either inactivated or denatured iron was released indicating it is essential for TAO activity. Moreover, this data has established biochemically the validity of predicting the presence of a diiron center from amino acid sequence data, not only in AOX but also in other membrane-bound diiron carboxylate proteins including 5-demethoxyquinone hydroxylase (CLK-1/Coq7) (which also has the diiron binding motif EXXH). It is of interest to note that both AOX and CLK-1/Coq7 utilize ubiquinol as substrate and both are involved in respiration [42–44].

4.3. Kinetic analysis

The inclusion of C10E8 in the assay was found to be critical for the kinetic analysis of TAO and the evaluation of inhibitors. In Table 3, we have calculated fundamental kinetic parameters of TAO and compared them to those of *E. coli* cytochrome *bo* oxidase complex and *S. cerevisiae* ubiquinol–cytochrome *c* reductase [45]. These kinetic constants provide a molecular rationale on how the alternative pathway can effectively compete with other terminal oxidases, although caution must be exercised in the interpretation of this data as it is derived from experiments performed under non-physiological conditions and substrates. Nevertheless Table 3 indicates that TAO has a calculated k_{cat} of $415 \pm 19\ s^{-1}$ (on the basis that the purity of rTAO is 95%), which is slightly higher than that of the cytochrome *bo* oxidase complex ($313\ s^{-1}$), yeast ubiquinol–cytochrome *c* reductase ($153\ s^{-1}$) and previous values reported for the plant AOX ($186\ s^{-1}$), but considerably less than that calculated for cytochrome *c* oxidase ($770\ s^{-1}$) [45–48]. Taking into account that the value of the specificity constant (k_{cat}/K_m) of enzymatic reactions is known to be less than $10^9\ M^{-1}\ s^{-1}$ (from the perspective of diffusion limited access of substrates [49]), it is apparent from Table 3 that both cytochrome *bo* oxidase and TAO have quite high and comparable catalytic activities. These values suggest that the activation energy of both quinol oxidase reactions are similar and furthermore that the quinol oxidase activity of TAO is thermodynamically "alternative" to that of the cytochrome *bo* complex. In contrast however, TAO does not appear to compete effectively with the bc_1 complex in terms of specificity constant and, if the plant AOX possesses a similar specificity constant to that of TAO, it would suggest that plant alternative oxidase activity would be severely curtailed unless the conventional respiratory chain is limited either through inhibition (which appears to be the case under 'stressed conditions') or through down regulation as appears to be the case in thermogenic tissues [12,50,51].

Interestingly ubiquinol-2 oxidation by rTAO showed substrate inhibition at concentrations above 100 μM in a manner similar to that observed when the heterodimeric terminal ubiquinol oxidase of *E. coli*, cytochrome *bd* oxidized ubiquinol-2 as substrate [52]. A lower K_m value of ubiquinol-2 than that of ubiquinol-1 might be related not only to its hydrophobicity but also could be a function of the isoprenoid chain. The peculiar kinetics of ubiquinol-2 might be attributed to the following two points; 1) competition for the ubiquinol-2 oxidation site between the substrate and the product, and 2) the presence of inactive intermediates of the enzyme related to the precise catalytic mechanism.

Kinetic analysis of the mechanism of inhibition by the specific TAO inhibitor ascofuranone (Sup. Fig. 5) indicates that it is a mixed-type inhibitor with respect to ubiquinol-1. The discrepancy between the mixed inhibition observed in this report and competitive inhibition as reported in our previous study [36] might be due to the different assay conditions used in the experiments described in this paper. In the previous study, the kinetic parameters were based on apparent values because enzymatic activity was calculated without detergents and hence only low ranges of ubiquinol-1 concentrations (0.01 K_m–0.3 K_m) could be used. In contrast, the kinetic parameters reported in the current study were determined with much higher reliability since in the presence of C10E8, a much wider range of ubiquinol-1 (0.4 K_m–1.7 K_m) could be used.

Table 3
Kinetic parameters of quinol oxidases (with respect to ubiquinol-1).

	K_m (μM)	V_{max} (μmol/min/mg protein)	k_{cat} (s^{-1})	k_{cat}/K_m ($\mu M^{-1}\ s^{-1}$)
TAO[a]	338 ± 23.2	601 ± 27.0	415 ± 19	1.2
Cyt *bo* oxidase[b]	61	–	313	5.2
Ubiquinol-cyt *c* reductase[c]	13	–	220	16.9

The k_{cat} value of cytochrome *c* oxidase is $k_{cat} = 770\ (s^{-1})$ [46].
All the k_{cat} values listed here were obtained by dividing the V_{max} by the concentration of the enzymes (mol/mg protein).
[a] This study.
[b] *E. coli* cytochrome *bo* oxidase as in Sakamoto et al. [47].
[c] Ubiquinol–cytochrome *c* reductase from bovine heart as in Fato et al. [45].

4.4. Unique feature of AOX

AOX is found in various organisms and recent genome database searches have also identified AOX in different phyla of the Animalia kingdom (Mollusca, Nematoda and Chordata) [17]. It has been suggested that since AOX is absent from mammalian tissues TAO could be a chemotherapeutic target, since it functions in the bloodstream form of *T. brucei* as the only terminal oxidase and hence is essential for the survival of trypanosomes [5,6]. As an AOX protein has also been identified in *Cryptosporidium parvum* [53,54], which causes diarrheal disease cryptosporidiosis, and the recombinant *C. parvum* AOX is also sensitive to ascofuranone and as a result suggests that not only could AOX be a potential drug target in a number of parasites but furthermore ascofuranone could be used to treat a number of infections since this compound shows potent, broad-spectrum antimicrobial activity [53].

In addition to this clinical application, there is considerable interest in the unique characteristics of the enzyme since the functions and properties of TAO are clearly distinct from those of other bacterial quinol oxidases. TAO is a cytochrome-independent and cyanide-insensitive quinol oxidase, whereas cytochrome *bo* and *bd* complexes are cytochrome-dependent and cyanide-sensitive quinol oxidases [34,35]. Furthermore, TAO has various other physiological roles in *T. brucei*; the cytochrome and alternative pathways are both active and functional in the procyclic forms [55] in addition to the bloodstream form, thereby possibly providing metabolic flexibility under changing environmental conditions. TAO activity also appears to regulate the expression of one of the major surface coat proteins, GPEET, in the procyclic form [56], and in addition may regulate the observed programmed cell death-like phenomena in the bloodstream forms [57].

5. Conclusions

The primary aim of our research on TAO is to elucidate the interaction between the enzyme and its substrate or inhibitor, which hopefully could act as a structural guide for ongoing drug development. In addition to the knowledge obtained from this study, further studies on the inhibitory kinetics and structure–activity relationship of ascofuranone derivatives, along with mutational analyses of TAO [27,29] and X-ray structure analysis will undoubtedly have considerable implications with respect to our understanding of how the enzyme interacts with its substrate and inhibitors. A three-dimensional structure of TAO with and without ascofuranone should also shed light on the inhibitory mechanism of this potent drug, which according to this study occurs via a mixed-type inhibition. Such further insights about the interaction between ascofuranone and the enzyme will hopefully lead to a more rational design of more potent and safe anti-trypanosomal drugs.

Acknowledgements

This work was supported in part by Grant-in-aid for Young Scientists (B) 21790402 (to YK), Grant-in-Aid for Scientific Research (C) 21590467 (to YY), Creative Scientific Research Grant 18GS0314 (to KK), Grant-in-aid for Scientific Research on Priority Areas 18073004 (to KK) from the Japanese Society for the Promotion of Science, and Targeted Proteins Research Program (to KK) from the

Japanese Ministry of Education, Science, Culture, Sports and Technology (MEXT) and a grant for research to promote the development of anti-AIDS pharmaceuticals from the Japan Health Sciences Foundation (to KK). ALM gratefully acknowledges BBSRC for financial support and with KK the Prime Ministers Initiative 2 (Connect) fund for collaborative twinning.

Appendix A. Supplementary data

Supplementary data associated with this article can be found, in the online version, at doi:10.1016/j.bbabio.2009.12.021.

References

[1] WHO, Control and surveillance of African trypanosomiasis, Report of a WHO Expert Committee, World Health Organ Tech Rep Ser, vol. 881, 1998, pp. 1–114, I–VI.
[2] C.E. Clayton, P. Michels, Metabolic compartmentation in African trypanosomes, Parasitol. Today 12 (1996) 465–471.
[3] F.R. Opperdoes, P. Borst, S. Bakker, W. Leene, Localization of glycerol-3-phosphate oxidase in the mitochondrion and particulate NAD+-linked glycerol-3-phosphate dehydrogenase in the microbodies of the bloodstream form to *Trypanosoma brucei*, Eur. J. Biochem. 76 (1977) 29–39.
[4] A.B. Clarkson Jr., E.J. Bienen, G. Pollakis, R.W. Grady, Respiration of bloodstream forms of the parasite *Trypanosoma brucei brucei* is dependent on a plant-like alternative oxidase, J. Biol. Chem. 264 (1989) 17770–17776.
[5] M. Chaudhuri, R.D. Ott, G.C. Hill, Trypanosome alternative oxidase: from molecule to function, Trends Parasitol. 22 (2006) 484–491.
[6] C. Nihei, Y. Fukai, K. Kita, Trypanosome alternative oxidase as a target of chemotherapy, Biochim. Biophys. Acta 1587 (2002) 234–239.
[7] N. Minagawa, Y. Yabu, K. Kita, K. Nagai, N. Ohta, K. Meguro, S. Sakajo, A. Yoshimoto, An antibiotic, ascofuranone, specifically inhibits respiration and in vitro growth of long slender bloodstream forms of *Trypanosoma brucei brucei*, Mol. Biochem. Parasitol. 84 (1997) 271–280.
[8] Y. Yabu, A. Yoshida, T. Suzuki, C. Nihei, K. Kawai, N. Minagawa, T. Hosokawa, K. Nagai, K. Kita, N. Ohta, The efficacy of ascofuranone in a consecutive treatment on *Trypanosoma brucei brucei* in mice, Parasitol. Int. 52 (2003) 155–164.
[9] Y. Yabu, T. Suzuki, C. Nihei, N. Minagawa, T. Hosokawa, K. Nagai, K. Kita, N. Ohta, Chemotherapeutic efficacy of ascofuranone in *Trypanosoma vivax*-infected mice without glycerol, Parasitol. Int. 55 (2006) 39–43.
[10] M. Chaudhuri, W. Ajayi, S. Temple, G.C. Hill, Identification and partial purification of a stage-specific 33 kDa mitochondrial protein as the alternative oxidase of the *Trypanosoma brucei brucei* bloodstream trypomastigotes, J. Eukaryot. Microbiol. 42 (1995) 467–472.
[11] A.L. Moore, J.N. Siedow, The regulation and nature of the cyanide-resistant alternative oxidase of plant mitochondria, Biochim. Biophys. Acta 1059 (1991) 121–140.
[12] A.L. Moore, M.S. Albury, Further insights into the structure of the alternative oxidase: from plants to parasites, Biochem. Soc. Trans. 36 (2008) 1022–1026.
[13] J.N. Siedow, A.L. Umbach, The mitochondrial cyanide-resistant oxidase: structural conservation amid regulatory diversity, Biochim. Biophys. Acta 1459 (2000) 432–439.
[14] T. Joseph-Horne, D.W. Hollomon, P.M. Wood, Fungal respiration: a fusion of standard and alternative components, Biochim. Biophys. Acta 1504 (2001) 179–195.
[15] A. McDonald, G. Vanlerberghe, Branched mitochondrial electron transport in the Animalia: presence of alternative oxidase in several animal phyla, IUBMB Life 56 (2004) 333–341.
[16] A.E. McDonald, G.C. Vanlerberghe, Alternative oxidase and plastoquinol terminal oxidase in marine prokaryotes of the Sargasso Sea, Gene 349 (2005) 15–24.
[17] A.E. McDonald, G.C. Vanlerberghe, J.F. Staples, Alternative oxidase in animals: unique characteristics and taxonomic distribution, J. Exp. Biol. 212 (2009) 2627–2634.
[18] D.A. Berthold, M.E. Andersson, P. Nordlund, New insight into the structure and function of the alternative oxidase, Biochim. Biophys. Acta 1460 (2000) 241–254.
[19] C. Affourtit, M.S. Albury, P.G. Crichton, A.L. Moore, Exploring the molecular nature of alternative oxidase regulation and catalysis, FEBS Lett. 510 (2002) 121–126.
[20] D.P. Maxwell, Y. Wang, L. McIntosh, The alternative oxidase lowers mitochondrial reactive oxygen production in plant cells, Proc. Natl. Acad. Sci. U. S. A. 96 (1999) 8271–8276.
[21] A.L. Moore, M.S. Albury, P.G. Crichton, C. Affourtit, Function of the alternative oxidase: is it still a scavenger? Trends Plant Sci. 7 (2002) 478–481.
[22] S. Mackenzie, L. McIntosh, Higher plant mitochondria, Plant Cell 11 (1999) 571–586.
[23] J.N. Siedow, A.L. Umbach, A.L. Moore, The active site of the cyanide-resistant oxidase from plant mitochondria contains a binuclear iron center, FEBS Lett. 362 (1995) 10–14.
[24] M.E. Andersson, P. Nordlund, A revised model of the active site of alternative oxidase, FEBS Lett. 449 (1999) 17–22.
[25] M.S. Albury, C. Affourtit, A.L. Moore, A highly conserved glutamate residue (Glu-270) is essential for plant alternative oxidase activity, J. Biol. Chem. 273 (1998) 30301–30305.
[26] M. Chaudhuri, W. Ajayi, G.C. Hill, Biochemical and molecular properties of the *Trypanosoma brucei* alternative oxidase, Mol. Biochem. Parasitol. 95 (1998) 53–68.
[27] W.U. Ajayi, M. Chaudhuri, G.C. Hill, Site-directed mutagenesis reveals the essentiality of the conserved residues in the putative diiron active site of the trypanosome alternative oxidase, J. Biol. Chem. 277 (2002) 8187–8193.
[28] M.S. Albury, C. Affourtit, P.G. Crichton, A.L. Moore, Structure of the plant alternative oxidase. Site-directed mutagenesis provides new information on the active site and membrane topology, J. Biol. Chem. 277 (2002) 1190–1194.
[29] K. Nakamura, K. Sakamoto, Y. Kido, Y. Fujimoto, T. Suzuki, M. Suzuki, Y. Yabu, N. Ohta, A. Tsuda, M. Onuma, K. Kita, Mutational analysis of the *Trypanosoma vivax* alternative oxidase: the $E(X)_6Y$ motif is conserved in both mitochondrial alternative oxidase and plastid terminal oxidase and is indispensable for enzyme activity, Biochem. Biophys. Res. Commun. 334 (2005) 593–600.
[30] D.A. Berthold, N. Voevodskaya, P. Stenmark, A. Graslund, P. Nordlund, EPR studies of the mitochondrial alternative oxidase. Evidence for a diiron carboxylate center, J. Biol. Chem. 277 (2002) 43608–43614.
[31] A.L. Moore, J.E. Carre, C. Affourtit, M.S. Albury, P.G. Crichton, K. Kita, P. Heathcote, Compelling EPR evidence that the alternative oxidase is a diiron carboxylate protein, Biochim. Biophys. Acta 1777 (2008) 327–330.
[32] A. Maréchal, Y. Kido, K. Kita, A.L. Moore, P.R. Rich, Identification of three redox states of recombinant *Trypanosoma brucei* alternative oxidase by FTIR spectroscopy and electrochemistry, J. Biol. Chem. 284 (2009) 31827–31833.
[33] Y. Fukai, H. Amino, H. Hirawake, Y. Yabu, N. Ohta, N. Minagawa, S. Sakajo, A. Yoshimoto, K. Nagai, S. Takamiya, S. Kojima, K. Kita, Functional expression of the ascofuranone-sensitive *Trypanosoma brucei brucei* alternative oxidase in the cytoplasmic membrane of *Escherichia coli*, Comp. Biochem. Physiol. C Pharmacol. Toxicol. Endocrinol. 124 (1999) 141–148.
[34] K. Kita, K. Konishi, Y. Anraku, Terminal oxidases of *Escherichia coli* aerobic respiratory chain. I. Purification and properties of cytochrome b_{562}-*o* complex from cells in the early exponential phase of aerobic growth, J. Biol. Chem. 259 (1984) 3368–3374.
[35] K. Kita, K. Konishi, Y. Anraku, Terminal oxidases of *Escherichia coli* aerobic respiratory chain. II. Purification and properties of cytochrome b_{558}-*d* complex from cells grown with limited oxygen and evidence of branched electron-carrying systems, J. Biol. Chem. 259 (1984) 3375–3381.
[36] C. Nihei, Y. Fukai, K. Kawai, A. Osanai, Y. Yabu, T. Suzuki, N. Ohta, N. Minagawa, K. Nagai, K. Kita, Purification of active recombinant trypanosome alternative oxidase, FEBS Lett. 538 (2003) 35–40.
[37] O. Maglio, F. Nastri, V. Pavone, A. Lombardi, W.F. DeGrado, Preorganization of molecular binding sites in designed diiron proteins, Proc. Natl. Acad. Sci. U. S. A. 100 (2003) 3772–3777.
[38] M.P. Hendrich, E. Munck, B.G. Fox, J.D. Lipscomb, Integer-spin Epr studies of the fully reduced methane monooxygenase hydroxylase component, J. Am. Chem. Soc. 112 (1990) 5861–5865.
[39] W.A. van den Berg, A.A. Stevens, M.F. Verhagen, W.M. van Dongen, W.R. Hagen, Overproduction of the prismane protein from *Desulfovibrio desulfuricans* ATCC 27774 in *Desulfovibrio vulgaris* (Hildenborough) and EPR spectroscopy of the [6Fe–6S] cluster in different redox states, Biochim. Biophys. Acta 1206 (1994) 240–246.
[40] M. Hoefnagel, P.R. Rich, Q. Zhang, J.T. Wiskich, Substrate kinetics of the plant mitochondrial alternative oxidase and the effects of pyruvate, Plant Physiol. 115 (1997) 1145–1153.
[41] Y. Kido, T. Shiba, D.K. Inaoka, K. Sakamoto, T. Nara, T. Aoki, T. Honma, A. Tanaka, M. Inoue, S. Matsuoka, A. Moore, S. Harada, K. Kita, Crystallization and preliminary crystallographic analysis of cyanide-insensitive alternative oxidase from *Trypanosoma brucei brucei*, Acta. Crystallogr. Sect. F Struct. Biol. Cryst. Commun, doi:10.1107/S1744309109054062.
[42] H. Miyadera, H. Amino, A. Hiraishi, H. Taka, K. Murayama, H. Miyoshi, K. Sakamoto, N. Ishii, S. Hekimi, K. Kita, Altered quinone biosynthesis in the long-lived clk-1 mutants of *Caenorhabditis elegans*, J. Biol. Chem. 276 (2001) 7713–7716.
[43] P. Stenmark, J. Grunler, J. Mattsson, P.J. Sindelar, P. Nordlund, D.A. Berthold, A new member of the family of di-iron carboxylate proteins. Coq7 (clk-1), a membrane-bound hydroxylase involved in ubiquinone biosynthesis, J. Biol. Chem. 276 (2001) 33297–33300.
[44] D.A. Berthold, P. Stenmark, Membrane-bound diiron carboxylate proteins, Ann. Rev. Plant Biol. 54 (2003) 497–517.
[45] R. Fato, M. Cavazzoni, C. Castelluccio, G. Parenti Castelli, G. Palmer, M. Degli Esposti, G. Lenaz, Steady-state kinetics of ubiquinol-cytochrome c reductase in bovine heart submitochondrial particles: diffusional effects, Biochem. J. 290 (1993) 225–236 K.
[46] H. Witt, F. Malatesta, F. Nicoletti, M. Brunori, B. Ludwig, Tryptophan 121 of subunit II is the electron entry site to cytochrome-*c* oxidase in *Paracoccus denitrificans*. Involvement of a hydrophobic patch in the docking reaction, J. Biol. Chem. 273 (1998) 5132–5136.
[47] Sakamoto, H. Miyoshi, M. Ohshima, K. Kuwabara, K. Kano, T. Akagi, T. Mogi, H. Iwamura, Role of the isoprenyl tail of ubiquinone in reaction with respiratory enzymes: studies with bovine heart mitochondrial complex I and *Escherichia coli bo*-type ubiquinol oxidase, Biochemistry 37 (1998) 15106–15113.
[48] M.H.N. Hoefnagel, J.T. Wiskich, S.A. Madgwick, Z. Patterson, W. Oettmeier, P.R. Rich New, Inhibitors of the ubiquinol oxidase of higher plant mitochondria, Eur. J. Biochem. 233 (1995) 531–537.
[49] R.A. Alberty, G.G. Hammes, Application of the theory of diffusion-controlled reactions to enzyme kinetics, J. Phys. Chem. 62 (1958) 154–159.
[50] R. Clifton, A.H. Millar, J. Whelan, Alternative oxidases in Arabidopsis: a comparative analysis of differential expression in the gene family provides new insights into function of non-phosphorylating bypasses, Biochim. Biophys. Acta 1757 (2006) 730–741.
[51] A.M. Wagner, K. Krab, M.J. Wagner, A.L. Moore, Regulation of thermogenesis in flowering Araceae: the role of the alternative oxidase, Biochim. Biophys. Acta 1777 (2008) 993–1000.

[52] K. Sakamoto, H. Miyoshi, K. Takegami, T. Mogi, Y. Anraku, H. Iwamura, Probing substrate binding site of the *Escherichia coli* quinol oxidases using synthetic ubiquinol analogues, J. Biol. Chem. 271 (1996) 29897–29902.
[53] T. Suzuki, T. Hashimoto, Y. Yabu, Y. Kido, K. Sakamoto, C. Nihei, M. Hato, S. Suzuki, Y. Amano, K. Nagai, T. Hosokawa, N. Minagawa, N. Ohta, K. Kita, Direct evidence for cyanide-insensitive quinol oxidase (alternative oxidase) in apicomplexan parasite *Cryptosporidium parvum*: phylogenetic and therapeutic implications, Biochem. Biophys. Res. Commun. 313 (2004) 1044–1052.
[54] C.W. Roberts, F. Roberts, F.L. Henriquez, D. Akiyoshi, B.U. Samuel, T.A. Richards, W. Milhous, D. Kyle, L. McIntosh, G.C. Hill, M. Chaudhuri, S. Tzipori, R. McLeod, Evidence for mitochondrial-derived alternative oxidase in the apicomplexan parasite *Cryptosporidium parvum*: a potential anti-microbial agent target, Int. J. Parasitol. 34 (2004) 297–308.
[55] R. Walker Jr., L. Saha, G.C. Hill, M. Chaudhuri, The effect of over-expression of the alternative oxidase in the procyclic forms of *Trypanosoma brucei*, Mol. Biochem. Parasitol. 139 (2005) 153–162.
[56] E. Vassella, M. Probst, A. Schneider, E. Studer, C.K. Renggli, I. Roditi, Expression of a major surface protein of *Trypanosoma brucei* insect forms is controlled by the activity of mitochondrial enzymes, Mol. Biol. Cell 15 (2004) 3986–3993.
[57] A. Tsuda, W.H. Witola, K. Ohashi, M. Onuma, Expression of alternative oxidase inhibits programmed cell death-like phenomenon in bloodstream form of *Trypanosoma brucei rhodesiense*, Parasitol. Int. 54 (2005) 243–251.

Author's personal copy

FEBS Letters 583 (2009) 1446–1450

FEBS Letters

journal homepage: www.FEBSLetters.org

The *Plasmodium* HU homolog, which binds the plastid DNA sequence-independent manner, is essential for the parasite's survival

Narie Sasaki [a,b], Makoto Hirai [c], Katsura Maeda [b], Ryoko Yui [a], Kie Itoh [d], Syoko Namiki [a], Teppei Morita [a], Masayuki Hata [e], Kimiko Murakami-Murofushi [b], Hiroyuki Matsuoka [c], Kiyoshi Kita [e], Shigeharu Sato [f,*]

[a] *Division of Biological Science, Graduate School of Science, Nagoya University, Nagoya 464-8602, Japan*
[b] *Department of Biology, Faculty of Science, Ochanomizu University, Tokyo 112-0012, Japan*
[c] *Division of Medical Zoology, Department of Infection and Immunity, Jichi Medical University School of Medicine, Shimotsuke 329-0498, Japan*
[d] *Department of Integrated Biosciences, Graduate School of Frontier Sciences, University of Tokyo, 5-1-5 Kashiwanoha, Kashiwa 277-8562, Japan*
[e] *Department of Biomedical Chemistry, Graduate School of Medicine, The University of Tokyo, Tokyo 113-0033, Japan*
[f] *Division of Parasitology, MRC National Institute for Medical Research, London NW7 1AA, UK*

ARTICLE INFO

Article history:
Received 27 February 2009
Revised 26 March 2009
Accepted 31 March 2009
Available online 7 April 2009

Edited by Michael Ibba

Keywords:
DNA binding protein
HU
Knock-out
Plastid
Plasmodium berghei
Plasmodium falciparum

ABSTRACT

The nuclear genome of the human malaria parasite *Plasmodium falciparum* encodes a homolog of the bacterial HU protein (PfHU). In this study, we characterised PfHU's physiological function. PfHU, which is targeted exclusively to the parasite's plastid, bound its natural target – the plastid DNA – sequence-independently and complemented lack of HU in *Escherichia coli*. The HU gene could not be knocked-out from the genome of *Plasmodium berghei*, implying that HU is important for the parasite's survival. As the human cell lacks the HU homolog, PfHU is a potential target for drugs to control malaria.
© 2009 Federation of European Biochemical Societies. Published by Elsevier B.V. All rights reserved.

1. Introduction

Apicomplexan parasites such as the human malaria parasite *Plasmodium falciparum* have a vestigial secondary plastid that is often called the apicoplast [1]. Despite being non-photosynthetic, the apicomplexan plastid is indispensable for the parasite because the organelle is involved in essential metabolism such as isoprenoid biosynthesis [2]. The *P. falciparum* plastid contains its own genomic DNA which is 35 kb in size and extremely rich in A + T (86%) [1]. Almost all proteins encoded by the plastid DNA (ptDNA) are involved in either transcription or translation. Nevertheless, the plastid genome encodes at least one gene whose expression is critical for the parasite's survival, and drugs affecting bacterial type gene expression often cause the delayed death phenotype of the parasite [3].

In the plastid, genomic DNA is assembled into a compact, highly organised structure, the nucleoid [4], like in bacteria from which the plastid has evolved. Bacterial nucleoid formation depends on a group of bacterial histone-like DNA binding proteins (BHLs). The HU protein, which binds DNA in a sequence non-specific manner and bends the bound DNA, is the most abundant BHL in the bacterial cell [5]. *Escherichia coli* HU is a heterodimer of two highly homologous subunits HUα and HUβ, which are encoded by *hupA* and *hupB*, respectively [6]. HU is ubiquitously distributed among bacteria and this suggests that the protein is critical in bacterial nucleoid formation. In addition to an architectural role, HU is also involved in other cellular functions such as initiation of replication [7], transcriptional regulation [8] and DNA recombination [9] in *E. coli*.

Although the plastids of the photosynthetic eukaryotes are descendents of bacteria, their original, bacterial components have been gradually replaced to eukaryotic factors of equivalent function during the course of evolution. Today, the plastid HU homolog is only found in some algal species and apicomplexans [4]. The algal HUs such as those of *Cyanidioschyzon merolae* [10] and *Guillardia theta* [11] are capable of rescuing bacterial HU null mutants

Abbreviations: BHL, bacterial histone-like DNA binding protein; ptDNA, plastid DNA

* Corresponding author. Fax: +44 20 8816 2730.
E-mail address: ssato@nimr.mrc.ac.uk (S. Sato).

0014-5793/$36.00 © 2009 Federation of European Biochemical Societies. Published by Elsevier B.V. All rights reserved.
doi:10.1016/j.febslet.2009.03.071

Author's personal copy

from its abnormal phenotype. The HU of *G. theta* bends DNA to which it binds [11], suggesting that this protein is critical in the formation of the nucleoid in this alga's plastid.

Recently, Ram et al. reported that the nuclear genome of *P. falciparum* encodes a HU homolog (PfHU) that is probably involved in DNA compaction in the plastid [12]. They found PfHU doesn't exhibit the DNA-bending activity in vitro and attributed this to the fact that the protein lacks the highly conserved proline residue at the position corresponding to P63 of *E. coli* HUα.

In this study, we investigated how PfHU binds the plastid DNA, whether the protein complements lack of HU in an *E. coli* null mutant, and whether HU protein is essential in the related rodent malaria parasite *P. berghei*, in order to characterise the physiological function of PfHU.

2. Materials and methods

2.1. DNA-mobility shift assay

The Recombinant PfHUs, PfHU53-189 and PfHU53-148 were prepared as described in Supplementary material. DNA fragments A1280, A1838, B1624 and B1880 were PCR-amplified from the parasite's ptDNA with a set of synthetic primers described by Singh et al. [13]; AB1677 was amplified with 5′-CTTTATATGGAGCTCGTCCT-3′ and 5′-CTGATTTATTACCTGTTGGT-3′. Fifty nanograms of each DNA fragment was incubated with each recombinant protein (0, 50, 100, 200, 400, and 800 ng) in the reaction buffer (20 mM Tris–HCl, pH 7.5, 0.4 mM EDTA, 20 mM NaCl, 0.4 mM DTT) for 3 h at room temperature before application to a 1% agarose gel and electrophoresis, then the gel was stained with ethidium bromide.

2.2. Complementation test

The *hupB*::Km^r locus of the HUβ$^-$ *E. coli* strain JR1671 was transduced to the HUα$^-$ strain JR1670 carrying *hupA*::Cm^r to generate a *hupAhupB* double mutant by P1 transduction [14]. A pQE50 (Qiagen)-base expression plasmid encoding PfHU53-189 without an affinity tag was constructed and the *hupAhupB* double mutant was transformed with a plasmid expressing the recombinant protein. The transformant was grown on LB supplemented with 50 μg/ml kanamycin and 50 μg/ml ampicillin. Neither chloramphenicol nor IPTG was added to the growth medium because the double mutant was sensitive to chroramphenicol [14] and the excess induction of PfHU53-189 was harmful for growth of the bacteria (data not shown).

2.3. Knock-out of the nuclear gene of Plasmodium berghei

To disrupt the HU gene of *P. berghei* (PB000792.02.0) through double-crossover homologous recombination, the plasmid pPbHU-KO was constructed from pBS-DHFR [15] following the method used to construct another targeting plasmid pPbGCS1-KO, which was successfully used to knock-out the GCS1 gene of the parasite [16] (details in Supplementary material). *P. berghei* ANKA clone 2.34 was separately transfected with pPbGCS1-KO or pPbHU-KO by electroporation, and recombinant parasites were selected with pyrimethamine.

3. Results

3.1. PfHU binds the plastid DNA sequence-independently

Ram and colleagues reported that PfHU exhibits the DNA binding activity that is predictable from the presence of a complete BHL domain in the protein [12]. They also reported that PfHU is localised to the plastid [12]. We confirmed the plastid-specific location of the protein by immuno-fluorescence microscopy using the anti-PfHU antibody (Supplementary Fig. S1). Therefore, the organellar genomic DNA in the plastid is the only natural target of the binding of PfHU. Ram and colleagues carried out chromatin immuno-precipitation (ChIP) assays and suggested that PfHU binds at least part of the organellar DNA [12], but no further analysis has been done. Thus, in order to characterise the physiological function of PfHU in detail, we analysed the protein's binding to different parts of the ptDNA by DNA-mobility shift assay using the recombinant protein.

Transfection experiments using yellow fluorescent protein (YFP) fused to Met1-Met82 of PfHU (PfHU-YFP) showed that the N-terminal sequence functions as the plastid targeting sequence (Supplementary Fig. S2). We prepared two differently truncated forms of the recombinant PfHU, PfHU53-189 and PfHU53-148; PfHU53-189 lacks the N-terminal unconserved sequence (M1-I52) whereas PfHU53-148 contains only the BHL domain (Fig. 1A). The apparent molecular mass of PfHU53-189 determined by Western blotting is almost the same as the natural PfHU present in the parasite (Supplementary Fig. S3). This suggests that the unconserved N-terminal sequence is removed from the mature form of PfHU, which is almost the same as PfHU53-189, when the protein is targeted to the plastid.

For this analysis, we selected five different regions of the ptDNA (Fig. 1B). Four of them – A1838, A1820, B1624 and B1880 – were chosen from those described in the previous report by Singh et al [13], as they are in close proximity of the DNA replication initiation sites (A1820), protein coding regions with tRNA genes' cluster (B1624 and B1880) and a part of a protein coding gene (A1838), respectively. In addition, another region AB1677, which contains the ends of both the two gene clusters, was selected as it is supposed to be important in termination of transcription.

A PCR fragment of each region was incubated with PfHU53-189 and separated by agarose gel electrophoresis (Fig. 1C). The result clearly showed that the protein affected the mobility of all the five fragments. Shift of the band was apparent even at a protein/DNA mass ratio = 1 but it was much more prominent when the ratio was higher. The protein added at the same mass ratio affected the mobility of each fragment equally. This indicates that PfHU53-189 binds these five DNA fragments regardless of their size and nucleotide sequence. This suggests that PfHU binds the ptDNA sequence without specificity.

Another experiment with PfHU53-148, which consists of only the BHL domain of PfHU, showed that this shorter form also binds the ptDNA sequence-independently, though the protein's affinity for each fragment seemed to be lower than that of PfHU53-189 (Fig. 1D). This implies that the BHL domain is sufficient for PfHU to bind the DNA and the unique C-terminal sequence stabilises the DNA–protein complex.

3.2. PfHU complements the HU-deficient E. coli mutant

Although neither of the two genes (*hupA* and *hupB*) encoding the two subunits of HU is essential for the survival of *E. coli* on LB at 37 °C, *hupAhupB* double mutants exhibit characteristic phenotypes such as filamentous morphology and sensitivity to the cold [17]. To characterise the function of PfHU further, a *hupAhupB* double mutant strain was transformed with the expression plasmid for PfHU53-189 and the effect of the expressed recombinant protein on the mutant's phenotypes investigated.

Unlike the HU$^+$ parent strain JR1669 that is short and homogeneous in size, the *hupAhupB* double mutant exhibits a characteristic filamentous phenotype (Fig. 2A). On the LB plate, the mutant forms visible colonies at 37 °C, but no visible colony is formed at 25 °C (Fig. 2B). By contrast, the transformants expressing

Author's personal copy

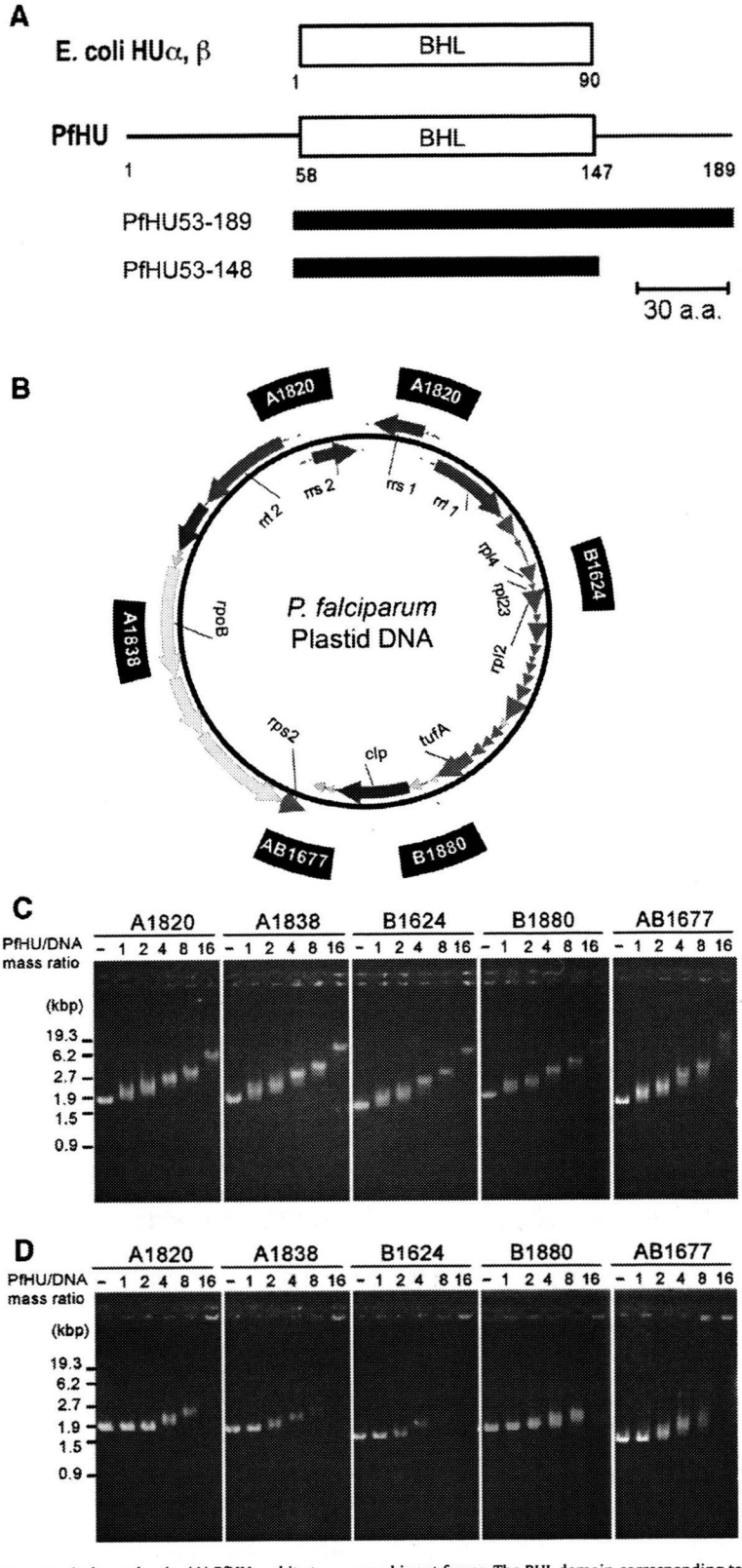

Fig. 1. PfHU binds the plastid DNA sequence-independently. (A) PfHU and its two recombinant forms. The BHL domain corresponding to the *E. coli* HU subunits is boxed. (B) Map of the plastid DNA of *P. falciparum*. The position of each DNA fragment used in the DNA-mobility shift assay is indicated outside the map. (C and D) DNA mobility shift assay. C, PfHU53-189; D, PfHU53-148. Note that the mobility of all fragments tested was similarly affected by each recombinant PfHU. The number of base pairs per one molecule of PfHU is 26 (PfHU53-189) or 18 (PfHU53-148), when the mass ratio of the protein to DNA is 1.

Author's personal copy

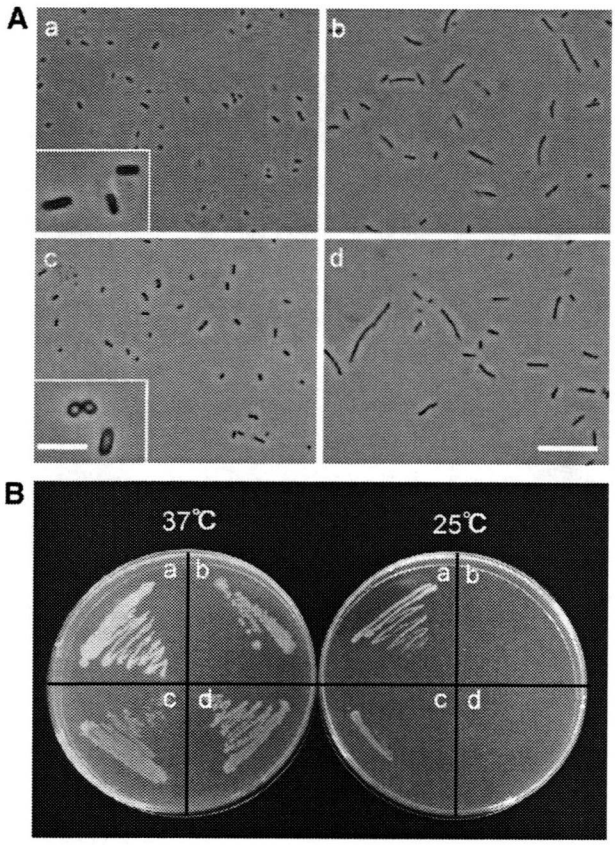

Fig. 2. PfHU complements the lack of HU in *E. coli*. (A) Phase-contrast micrographs of the HU$^+$ strain (a), the *hupAhupB* mutant (b), the *hupAhupB* mutant expressing PfHU53-189 (c) and the *hupAhupB* mutant carrying pQE50 (d). Scale bar: 5 μm. Inset, magnified view. Scale bar: 1 μm. (B) Growth of bacteria on LB plate at different temperature. Bacteria in each sector (a–d) were as in A. Each plate was incubated for 20 h (37 °C) or 40 h (25 °C).

PfHU53-189 were short in length and looked similar to the HU$^+$ parent strain (Fig 2Ac), and capable of forming robust colonies on the LB plate at both the permissive (37 °C) and the restrictive (25 °C) temperatures (Fig. 2B). The presence of the expression vector itself did not affect either the filamentous- or the cold-sensitive-phenotype of the double mutant. These results suggest that the PfHU53-189 functionally complements the deficiency of HU of the *hupAhupB* strain.

3.3. The HU gene is important for survival of the malaria parasite

Not only *P. falciparum* but other *Plasmodium* spp. have one gene for HU in the nuclear genome; for example, PB000792.02.0 (*PbHU*) is the gene of the rodent malaria parasite *P. berghei*. *Plasmodium* HUs are closely related to each other and the sequence alignment suggests that each *Plasmodium* HU has a plastid targeting sequence at the N terminus (Supplementary Fig. S4). This implies that all these *Plasmodium* HUs share the same physiological function(s). To investigate the importance of HU for *Plasmodium* spp., we constructed a targeting plasmid pPbHU-KO from pBS-DHFR [15] and attempted to disrupt the *HU* gene of *P. berghei* with the plasmid. Although the control experiment with a sister pBS-DHFR-based plasmid pPbGCS1-KO [16] easily generated the *PbGCS1* gene disruptant, we never obtained the *PbHU* knockout parasite in several repeated trials. This suggests that the *PbHU* locus is essential for the parasite's survival at least during the asexual blood stage, and that the gene is also indispensible for the survival of other species such as *P. falciparum*. Probably the HU protein encoded by the gene is important for the function and/or maintenance of the ptDNA of *Plasmodium* spp., though another possibility that the manipulation of this particular locus adversely affects the expression of other important genes [18] has not been ruled out yet.

4. Discussion

PfHU is a plastid protein and our mobility shift assay confirmed that PfHU's direct binding to the parasite's ptDNA is sequence-independent. These data imply that PfHU is involved in the assembly of the nucleoid in the plastid as an architectural protein. The filamentous phenotype of the *E. coli hupAhupB* mutant is attributed to perturbed expression of specific cell division genes [19] whereas the cold-sensitive phenotype of the mutant can be caused by unstable binding of DnaA to the binding sites in the chromosomal replication origin *oriC* [6,20]. Thus, data obtained by our complementation test suggest that PfHU adjusted the expression of genes determining bacterial shape and promoted initiation of chromosome replication by stabilising DnaA's binding to *oriC* in *E. coli*. It is questionable whether the *Plasmodium* plastid and *E. coli* share the same regulation systems for either gene expression or chromosome replication, but our data suggest that PfHU is capable to exhibits sequence-specific functions presumably by changing the architectural structure of ptDNA in the plastid.

The HU gene was impossible to knock-out from the genome of *P. berghei*, strongly suggesting that the *HU* gene is also likely indispensible for the survival of *P. falciparum*. Although it is hardly known how gene expression and replication of the organellar DNA are regulated in the *Plasmodium* plastid, PfHU is possibly involved in such sequence-dependent events in addition to general maintenance of ptDNA. Because a HU ortholog is absent from the humans, PfHU should be a promising target of the controlling drugs against malaria.

Acknowledgements

The authors thank Dr. J. Rouviere-Yaniv (Institut Pasteur, France) for providing us with *E. coli* strains JR1669, JR1670 and JR1671. This work was financially supported by the British Medical Research Council (MRC), and a Grant-in-Aid for Creative Scientific Research (18GS0314-01 to N.S. and 18GS0314 to K.K) and for Scientific Research (C) (20590426 to M.H) from Japanese Ministry of Education, Science, Culture, Sports, and Technology.

Appendix A. Supplementary data

Supplementary data associated with this article can be found, in the online version, at doi:10.1016/j.febslet.2009.03.071.

References

[1] Wilson, R.J.M. et al. (1996) Complete gene map of the plastid-like DNA of the malaria parasite *Plasmodium falciparum*. J. Mol. Biol. 261, 155–172.
[2] Ralph, S.A. et al. (2004) Tropical infectious diseases: metabolic maps and functions of the *Plasmodium falciparum* apicoplast. Nat. Rev. Microbiol. 2, 203–216.
[3] Dahl, E.L. and Rosenthal, P.J. (2008) Apicoplast translation, transcription and genome replication: targets for antimalarial antibiotics. Trends Parasitol. 24, 279–284.
[4] Sato, N., Terasawa, K., Miyajima, K. and Kabeya, Y. (2003) Organization, developmental dynamics, and evolution of plastid nucleoids. Int. Rev. Cytol. 232, 217–262.
[5] Swinger, K.K. and Rice, P.A. (2004) IHF and HU: flexible architects of bent DNA. Curr. Opin. Struct. Biol. 14, 28–35.
[6] Pettijohn, D.E. (1988) Histone-like proteins and bacterial chromosome structure. J. Biol. Chem. 263, 12793–12796.
[7] Bramhill, D. and Kornberg, A. (1988) A model for initiation at origins of DNA replication. Cell 54, 915–918.

Author's personal copy

[8] Aki, T. and Adhya, S. (1997) Repressor induced site-specific binding of HU for transcriptional regulation. EMBO J. 16, 3666–3674.
[9] Dri, A.M., Moreau, P.L. and Rouviere-Yaniv, J. (1992) Role of the histone-like proteins OsmZ and HU in homologous recombination. Gene 120, 11–16.
[10] Kobayashi, T., Takahara, M., Miyagishima, S.Y., Kuroiwa, H., Sasaki, N., Ohta, N., Matsuzaki, M. and Kuroiwa, T. (2002) Detection and localization of a chloroplast-encoded HU-like protein that organizes chloroplast nucleoids. Plant Cell 14, 1579–1589.
[11] Wu, H. and Liu, X.Q. (1997) DNA binding and bending by a chloroplast-encoded HU-like protein overexpressed in *Escherichia coli*. Plant Mol. Biol. 34, 339–343.
[12] Ram, E.V., Naik, R., Ganguli, M. and Habib, S. (2008) DNA organization by the apicoplast-targeted bacterial histone-like protein of *Plasmodium falciparum*. Nucleic Acids Res. 36, 5061–5073.
[13] Singh, D., Chaubey, S. and Habib, S. (2003) Replication of the *Plasmodium falciparum* apicoplast DNA initiates within the inverted repeat region. Mol. Biochem. Parasitol. 126, 9–14.
[14] Huisman, O., Faelen, M., Girard, D., Jaffe, A., Toussaint, A. and Rouviere-Yaniv, J. (1989) Multiple defects in *Escherichia coli* mutants lacking HU protein. J. Bacteriol. 171, 3704–3712.
[15] Dessens, J.T., Beetsma, A.L., Dimopoulos, G., Wengelnik, K., Crisanti, A., Kafatos, F.C. and Sinden, R.E. (1999) CTRP is essential for mosquito infection by malaria ookinetes. EMBO J. 18, 6221–6227.
[16] Hirai, M. et al. (2008) Male fertility of malaria parasites is determined by GCS1, a plant-type reproduction factor. Curr. Biol. 18, 607–613.
[17] Wada, M., Kano, Y., Ogawa, T., Okazaki, T. and Imamoto, F. (1988) Construction and characterization of the deletion mutant of *hupA* and *hupB* genes in *Escherichia coli*. J. Mol. Biol. 204, 581–591.
[18] Patankar, S., Munasinghe, A., Shoaibi, A., Cummings, L.M. and Wirth, D.F. (2001) Serial analysis of gene expression in *Plasmodium falciparum* reveals the global expression profile of erythrocytic stages and the presence of anti-sense transcripts in the malarial parasite. Mol. Biol. Cell 12, 3114–3125.
[19] Dri, A.M., Rouviere-Yaniv, J. and Moreau, P.L. (1991) Inhibition of cell division in *hupA hupB* mutant bacteria lacking HU protein. J. Bacteriol. 173, 2852–2863.
[20] Guo, L., Katayama, T., Seyama, Y., Sekimizu, K. and Miki, T. (1999) Isolation and characterization of novel cold-sensitive *dnaA* mutants of *Escherichia coli*. FEMS Microbiol. Lett. 176, 357–366.

Heat Inactivation of Fetal Bovine Serum

AfCS Procedure Protocol ID PP00000127
Version 1, 11/25/02

In this procedure, fetal bovine serum (FBS) is heated to 56 °C in a water bath to destroy heat-labile complement proteins prior to use in cell growth medium. This procedure is similar to that recommended by HyClone (HyClone Handling Serum procedure; 1-800 HYCLONE).

Heat Inactivation Procedure

1. Remove 500-ml bottle of FBS from –80 °C freezer and place in refrigerator to thaw overnight. Complete thawing of serum the following day by placing serum in a 37 °C water bath with a water level higher than the serum level in the bottle. Mix by inversion.
2. Once serum is completely thawed, incubate for an additional 15 min to allow serum to equilibrate with the 37 °C bath.
3. Raise the temperature setting of the bath to 56 °C. Use a timer to measure the 35 min needed for the temperature of the bath and serum to come to 56 °C. During this incubation, invert the bottle to mix the serum every 10 min. If necessary, allow an additional 5 min for bath to reach 56 °C.
4. Once bath reaches 56 °C, incubate serum for 30 min. Invert bottle every 10 min.
5. Remove serum from water bath and allow to cool at room temperature for 30 min. Reset water bath to the 37 °C mark.
6. Aliquot 50 ml of treated serum into conical tubes and store at 4 °C or freeze at –20 °C.

Reagents and Materials

Fetal bovine serum (FBS): GIBCO/Invitrogen; catalog no. 26140079

Conical tubes, 50 ml: Greiner; catalog no. 4943

Author: Richard Davis/Robert Hsueh

Date: 12/02/02

Approved: Paul Sternweis

BLOOD STAGE *PLASMODIUM FALCIPARUM* ANTIGENS INDUCE IMMUNOGLOBULIN CLASS SWITCHING IN HUMAN ENRICHED B CELL CULTURE

Pachuen Potup[1,2,3], Ratchanok Kumsiri[2], Shigeyuki Kano[4], Thareerat Kalambaheti[5], Sornchai Looareesuwan[6*], Marita Troye-Blomberg[7] and Yaowapa Maneerat[2]

[1]Department of Tropical Radioisotopes, [2]Department of Tropical Pathology, Faculty of Tropical Medicine, Mahidol University, Bangkok; [3]Department of Radiological Tecnology, Faculty of Allied Health Sciences, Naresuan University, Phitsanulok; [4]Department of Appropriate Technology Development and Transfer, Research Institute, International Medical Center of Japan, Tokyo, Japan; [5]Department of Microbiology and Immunology, [6]Department of Clinical Tropical Medicine, Faculty of Tropical Medicine, Mahidol University, Bangkok, Thailand; [7]Department of Immunology, Stockholm University, Stockholm, Sweden

Abstract. This study aimed to demonstrate class switch recombination (CSR) in heavy chain expressing immunoglobulin G (IgG) and IgE in human B cells after exposure to *Plasmodium falciparum* schizont lysate. Human B cells ($CD20^+CD27^-$) were cultured with crude *P. falciparum* antigen (cPfAg) and anti-CD40. On Day 4 post-exposure, total RNA from B cells was prepared and the occurrence of CSR from IgM to IgG and/or IgE was investigated by reverse transcription-polymerase chain reaction. Molecular markers to detect active CSR included enzyme activation-induced cytidine deaminase mRNA, γ and ε-germline transcripts (γ, ε-GLT), circle transcript (CT) and mature transcript (γ and ε-mRNA) expression. On Day 7 and Day 14 after exposure, levels of Igs in the culture supernatant were determined by enzyme-linked immunosorbent assay. Our findings showed that we could demonstrate cPfAg-stimulated B cells undergoing CSR by use of the expressed CSR markers and the increase in specific IgG and IgE indicating the potential of this approach in the study of CSR in *P. falciparum*-stimulated B cells.

INTRODUCTION

Human malaria still causes approximately 1 million deaths from 500 million malaria cases each year. *Plasmodium falciparum* is the major cause of severe and fatal malaria with complications, *eg*, coma from cerebral malaria, renal failure and severe anemia (Greenwood *et al*, 2008). Antibodies and T cells are among the immune factors thought to play a role in mediating protection and also pathology (Adams *et al*, 2002; Heddini, 2002). In *P. falciparum* infection serum levels of immunoglobulin M (IgM), IgG and IgE increase in individuals living in endemic areas (Perlmann *et al*, 2000; Calissano *et al*, 2003; Bereczky *et al*, 2004; Seka-Seka *et al*, 2004; Bolad *et al*, 2005;

Correspondence: Dr Yaowapa Maneerat, Department of Tropical Pathology, Faculty of Tropical Medicine, Mahidol University, 420/6 Ratchawithi Road, Bangkok 10400, Thailand.
Tel: 66 (0) 2354 9100-19 ext 1629; Fax: 66 (0) 2644 7938.
E-mail: tmymn@mahidol.ac.th
*Deceased